

## The adsorption of arsenic on magnetic iron oxide in aqueous solutions

Guiqiu Liu\*, Nairui Liu, Hefei Zhang, Lixi Zhang

School of Dynamics and Energy, Northwestern Polytechnical University, P. R. China  
Tel. +862988492440; Fax +862987293429; email: liu-guiqiu@tom.com

Received 24 September 2008; accepted 11 March 2010

---

### ABSTRACT

Iron oxides are widely used as adsorbents to remove pollutants because of their excellent surface activities and resultant significant adsorption capabilities. In an effort to study the adsorption and desorption behavior of arsenic in aqueous solutions containing magnetism iron oxide (MIO), solid–liquid separations were conducted in the laboratory using synthetically-prepared solutions. Results indicate that arsenic can be easily adsorbed and the adsorption can be described using Langmuir and Freundlich equation. It was determined that the capability of MIO for arsenic adsorption depended primarily on the surface activity of the adsorbent, pH of the solution, and arsenic speciation. Optimization adsorption was found to occur between pH 6.0 and 9.4 for arsenic (III) and pH less than 5.0 for arsenic (V). Adsorbed arsenic (V) could be easily desorbed from using a 10 percent solution of sodium hydroxide whereas arsenic (III) was found to be recalcitrant.

**Keywords:** Arsenic; Adsorption isotherm; Influencing factors; MIO

---

### 1. Introduction

Arsenic contamination can occur in aquatic and terrestrial environments due to the widespread application of pesticides, smelters, coal-fired power plants and dissolution of arsenic-enriched minerals [1]. Arsenic is a cancer causing substance which is predominantly present as inorganic species in natural water system. Long-term uptake of arsenic contaminated water causes liver, lung, kidney, bladder, skin and nerve tissue damages [2]. Therefore, it is urgent and important to remove arsenic and its compounds from wastewater and contaminated drinking water. Over the years many technologies have been developed for the removal of arsenic from aqueous environments. However, adsorption has emerged as a more popular alternative because of its simplicity and potential to offer a sludge-free operation [2,3]. According to

previous studies, iron oxides, including oxyhydroxides and hydroxides, such as amorphous hydrous ferric oxide (FeOOH), goethite ( $\alpha$ -FeOOH) and hematite ( $\alpha$ -Fe<sub>2</sub>O<sub>3</sub>), are promising effective adsorptive materials for arsenic removal from water due to its unusual surface activity and high adsorption affinity towards arsenic [4]. Although somewhat good results have been obtained, some deficiencies, such as poor performance for arsenite anion and difficulty with regeneration of spent adsorbents, still plagued the practice of arsenic removal from aqueous systems by the use of iron oxide. Furthermore, typically powered form of the adsorbents makes the separation of iron oxide from treated water inefficient [1–4]. In this study, the arsenic adsorption properties of the magnetism iron oxide compound (MIO) and the desorption of adsorbed arsenic were investigated. This adsorption material can be separated from water easily due to its magnetism nature and then be recycled after the regeneration.

---

\*Corresponding author

## 2. Materials and methods

### 2.1. Chemicals

All chemicals used were analytical reagent grade. Solutions were prepared from sodium arsenite ( $\text{NaAsO}_2$ ) for arsenic As(III) and sodium arsenate ( $\text{Na}_3\text{AsO}_4$ ) for arsenic As(V).

### 2.2. Preparation of MIO [5]

MIO was synthesized through the reaction of ferrous sulfate ( $\text{FeSO}_4 \cdot 7\text{H}_2\text{O}$ ) and ferric chloride ( $\text{FeCl}_3 \cdot 6\text{H}_2\text{O}$ ) in an alkali medium at  $90^\circ\text{C}$ . The synthesized material was washed with deionized water, and subsequently dried at  $100 \pm 5^\circ\text{C}$  inside an 101-4 electrothermal oven (Nanjing Suote Ganzao Shebei company, China), then ground in agate pot by manual and sieved through a 100 mesh sieve. The X-ray diffraction (XRD) analysis for the MIO crystallography was performed on a Rigaku (Japan) D/Max-3B diffractometer equipped with a monochromated Fe K $\alpha$  radiation. The monochromated radiation had a tube voltage of 40 kV, a tube current of 20 mA and the count time was 0.5 s/0.02 $^\circ$ .

### 2.3. Arsenic adsorption isotherm tests

To a series of 250 mL conical flasks were added 50 mL of 1–60 mg/L arsenic solutions and 50 mg of MIO. The pH was adjusted to 7.0 using 0.1 mol/L hydrochloric acid (HCl) or sodium hydroxide (NaOH) solutions. All samples were shaken at 250 rpm and room temperature ( $25 \pm 0.5^\circ\text{C}$ ) in a mechanical shaker (Changzhou Guohua Electric Appliance Co. Ltd) for 1 h, then were balanced 24 h. The suspension in each flask was filtered through a 0.45- $\mu\text{m}$  membrane filter and the filtrate was analyzed for As(III) and As(V) in 24 h. The amount of As(III) and As(V) uptake by MIO was calculated from the decrease of its concentration in solution. The data of arsenic adsorption were fitted with *Freundlich* and *Langmuir isotherm* models. The Langmuir isotherm is expressed as follows:

$$q_{\text{eq}} = \frac{bQ_{\text{max}}C_{\text{eq}}}{1 + bC_{\text{eq}}}$$

where  $Q_{\text{max}}$  (mg/mL) is the maximum adsorption capacity,  $C_{\text{eq}}$  (mmol/L) is the equilibrium solute concentration, and  $b$  is the equilibrium constant related to the energy of sorption (L/mmol).

The Freundlich isotherm is expressed as follows:

$$q_{\text{eq}} = KC_{\text{eq}}^{1/n}$$

where  $K$  is the empirical constant ((mg/mL)/(mmol/L) $^{1/n}$ ) and  $n$  the empirical constant

(dimensionless). A nonlinear regression was applied to obtain all Langmuir and Freundlich isotherm parameters.

Arsenic desorption Kinetics, in a 500 mL flask, 250 mL of 10% NaOH solution and 250 mg of saturated arsenic adsorbed MIO were mixed. The suspension was stirred at 250 rpm. The initial pH of the solution was 7.0, and the temperature was kept at  $25 \pm 0.5^\circ\text{C}$ . At regular time intervals an aliquot of 2 mL of supernatant was withdrawn for arsenic analysis.

Experiments were performed with the same procedure as described above to determine the effects of pH, ion strength and temperature on arsenic adsorption except that different solution conditions were controlled. 20 mg/L arsenic solutions with ion strength of 0.1 mol/L sodium chloride (NaCl) and with a series of initial pH at 3.0–10.0 were used in pH effect experiments. 20 mg/L arsenic solutions with a constant pH 7.0 and with a series ion strength at 0–2.0 mol/L NaCl were adopted in ion strength effect experiments. For temperature effect experiments, 20 mg/L arsenic solutions at different temperature of 20, 30, 40, 50, and  $60^\circ\text{C}$  were studied, and pH and ion strength were maintained at 7.0 and 0.1 mol/L NaCl, respectively. To ensure the accuracy, reliability and reproducibility of the collected data, all batch experiments were carried out in duplicate and the mean values are presented.

### 2.4. Methods of analysis

The solutions were spectrophotometrically analyzed for arsenic by the silver diethyldithiocarbamate method [6]. Total iron analysis was performed by 1,10-phenanthroline method as described in standard methods (APHA, 1985) [7]. Measurements of pH were made with a pH electrode and pHS-3C digit acidometer (Shanghai Rex Instrument Factory) calibrated with three buffer solutions at pH4.00, 6.86, and 9.18. The point of zero charge ( $\text{pH}_{\text{PZC}}$ ) were determined using a batch equilibration method [12].

## 3. Results and discussion

### 3.1. Characterization of MIO

The crystallographic structure can be identified by XRD pattern of the MIO sample in Fig. 1. The narrow and strong XRD reflections indicated that it was well crystallized. It was found that all the diffraction peaks could be well indexed to the inverse cubic spinel structure (JCPDS card No. 85-1436). Meanwhile, the crystal grains were perfect, evidenced by the sharp and strong diffraction peaks. And there are not any additional peaks in Fig. 1, showing that the MIO sample has high purity.

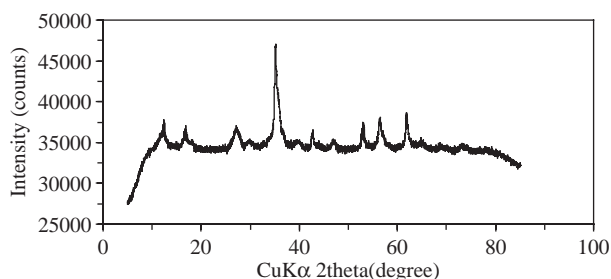


Fig. 1. Powder X-ray diffraction patterns of synthesized MIO.

### 3.2. Adsorption isotherms

Fig. 2 shows the adsorption isotherm curve of arsenic. More arsenic were adsorbed with the increasing equilibrium arsenic concentration in solution under the same conditions. The amount of As(V) adsorbed was slightly higher than that of As(III), which is disagreement previous research results that the difference is great between the adsorption of As(V) and As(III) on iron oxides [1,2,4]. The adsorption of arsenic with increasing equilibrium arsenic concentration can be divided into two stages, a rapid enhancement in arsenic adsorption as equilibrium concentration of arsenic is low, and a slow increase of that as equilibrium concentration of arsenic is high. This is possibly related to the degree of surface coverage of MIO by arsenic adsorbate. The potential of arsenic adsorption is relatively greater as the surface coverage is low because more activated adsorption sites are readily accessible, while the situations are on the contrary as the surface coverage is high because few unoccupied adsorption sites are retained. Therefore, the amounts of adsorbed arsenic increase only slowly as the equilibrium concentration of arsenic increase up to 23.2 and 25.1 mg/L for As(V) and As(III), respectively.

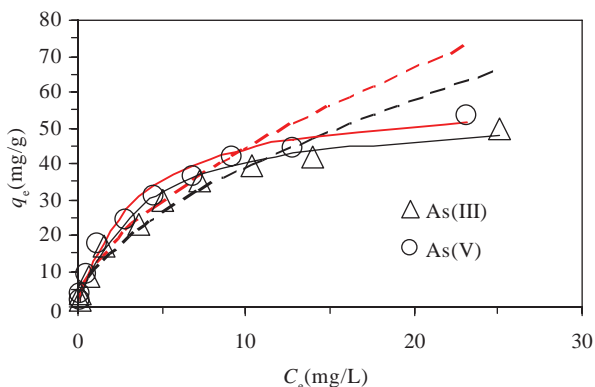


Fig. 2. Adsorption isotherm of arsenic on MIO. Solid lines indicate Freundlich equation prediction, dashed lines indicate Langmuir equation prediction.

As seen from Table 1, the adsorption data fitted Freundlich isotherm equation and Langmuir equation well. As the super activity and hydrolysis ability of As(V) are more than that of As(III), and the affinity of iron oxides to As(V) are stronger than to As(III), the amount of As(V) adsorption is more than that of As(III) on MIO. Alternatively, the specific structure of spinel structure compound oxides might be the second reason for the adsorption difference of As(III) and As(V) [8].

As shown in Fig. 3, the desorption of As(III) and As(V) on MIO is time dependent. The process of arsenic desorption is quick firstly, and then slowly approaches the equilibrium. The amount of arsenic desorbed is 60–80% of the overall desorption within 5 min. The desorption percentage of equilibrium is 66.3% for As(III) and 86.2% for As(V), indicating that the adsorbed arsenic can be effectively washed out with 10% NaOH solution, while the desorption percentage of As(V) is considerably greater than As(III).

### 3.3. Effect of pH on As(III) and As(V) adsorption on MIO

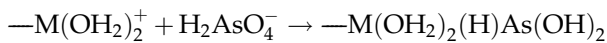
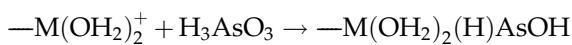
To determine the optimum pH for adsorption of arsenic over MIO, the uptake of arsenic as a function of pH was studied. The adsorption of arsenic in the range of pH 3–10 is shown in Fig. 4. The optimal pH for As(III) adsorption is observed in the range of 6–9.4. Beyond the optimal pH range, As(III) uptake significantly decreased. The optimal As(V) adsorption occurred under acidic conditions, and As(V) uptake significantly decreases as pH rises in the range of 5–10. When pH is above 5.8, MIO has higher adsorbing capability to As(V) than to As(III), but lower when pH less than 5.8.

Regardless the influence of electrostatic attraction, ionic exchange and the coordinate complexing on arsenic adsorption, it is most advantageous for arsenic adsorption when arsenic is in anion form and the adsorbent with positive charge. pH affects significantly the speciation of arsenic in solution and the surface charge of the solid particles [3]. Arsenate species and their corresponding stability pH values are  $\text{H}_3\text{AsO}_4$  (pH < 2),  $\text{H}_2\text{AsO}_4^-$  (pH 2–7),  $\text{HAsO}_4^{2-}$  (pH 7–11), and  $\text{AsO}_4^{3-}$  (pH > 12). Trivalent arsenic is stable as neutral  $\text{H}_3\text{AsO}_3$  at pH < 9, while  $\text{H}_2\text{AsO}_3^-$ ,  $\text{HAsO}_3^{2-}$ , and  $\text{AsO}_3^{3-}$  are stable species in the pH ranges of 9–12, 12–13, and >13, respectively. According to amphoteric dissociation theory, the surface of solid adsorbent is positively charged when the equilibrium pH values are below the point of zero charge ( $\text{pH}_{\text{PZC}}$ ), and it will be negatively charged when the equilibrium pH above  $\text{pH}_{\text{PZC}}$ . The adsorption reactions between arsenic species and metal oxides with  $\text{pH}_{\text{PZC}} > 7$  in acidic environment are as follows [9]:

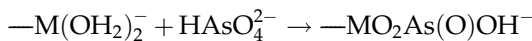
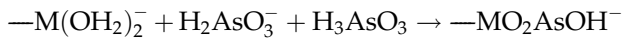
Table 1  
Coefficients of isothermal adsorption model fitting of arsenic removal

	Freundlich Equation			Langmuir Equation		
	$\log q_e = \log k + \frac{1}{n} \log C_e$	R	Se	R	Se	$q_{\max}$ mg/g
As(V)	$\log q_e = 0.5942 \log C_e + 1.0495$	0.9761	0.115	0.9937	0.015	58.8
As(III)	$\log q_e = 0.5832 \log C_e + 1.003$	0.9886	0.078	0.9932	0.018	55.2

where  $q_e$  is the uptake capacity,  $q_{\max}$  is the maximum uptake capacity,  $C_e$  is the equilibrium concentration,  $k$ , relative to the sorption capacity (mg/g),  $n$ , affinity coefficient,  $a$ , binding constant (L/mg),  $R$ , correlation coefficient and  $Se$  is the standard deviation.—



In neutral and alkaline environment, they are expressed as:



The  $pH_{zpc}$  obtained for MIO was pH 8.5. As the equilibrium pH increases up to pH 8.5, the decreased amount of arsenate adsorption is attributed to the decreasing electrostatic attraction between the surface of MIO and anionic arsenate species. The lower amount of arsenate adsorption at pH above 8.5 could be due to an increased repulsion between the negatively charged arsenate species and negatively charged surface sites. Since arsenite species have less negative charge compared to arsenate species at  $pH < 9$ , they do not exhibit as much repulsion, and as a result,

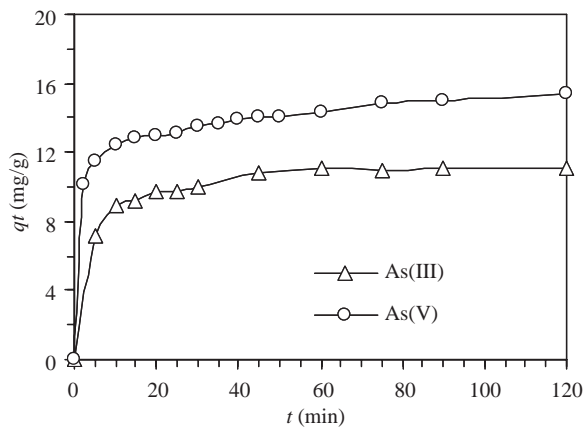


Fig. 3. Relationship between time and arsenic desorption in 10% NaOH solution at  $25 \pm 0.5^\circ\text{C}$ .

arsenite is preferably adsorbed by MIO in a wide pH range. An increase of negatively charged arsenite species and negatively charged surface sites might be the reason for the decrease in the adsorption yield above pH 9.4.

Tests show that the adsorption of As(III) at acidic pH is a hydrogen-release process, in contrast to a hydrogen-consuming process at alkaline pH. Thus, under separate acidic and alkaline conditions, further increase in acid and alkali strength will impel the adsorption reaction from the right side towards the left side and lead to the reduction of As(III) adsorption with increasing intensity of acidity and alkalinity. The favored As(III) adsorption at nearly neutral pH is a result of insignificant release (or consumption) of hydrogen during the reaction of  $H_3AsO_3$  and MIO.

#### 3.4. Effect of ion strength on As(III) and As(V) adsorption on MIO

Fig. 5 shows relationship between adsorption of As(III) & As(V) on MIO and ion strength. The amount of As(III) and As(V) adsorbed by MIO increase with the ionic strength of background electrolyte NaCl

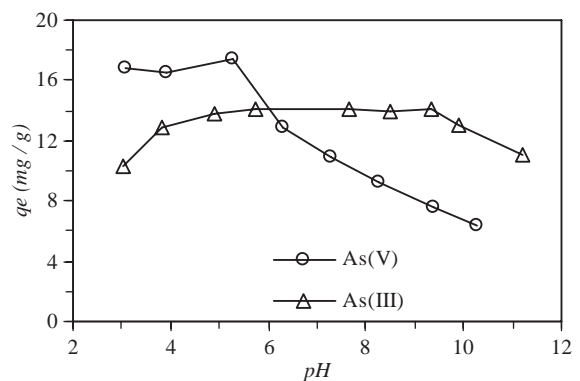


Fig. 4. Effects of pH on arsenic adsorption. The ionic strength of background electrolyte NaCl is 0.1 mol/L and the added arsenic is 20 mg/L.

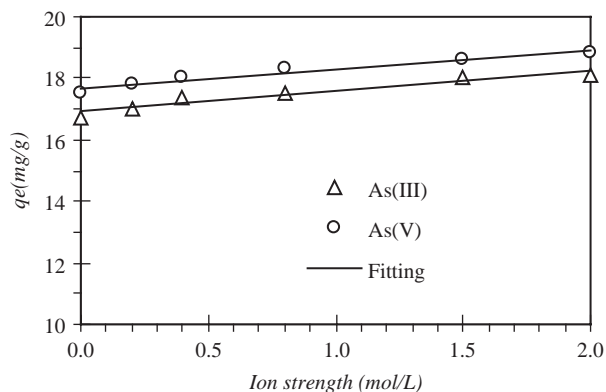


Fig. 5. Relationship between arsenic adsorption and ion strength. The solution pH is 7.0, and the added arsenic is 20 mg/L.

increasing, there are significantly correlative between arsenic adsorption and the concentration of NaCl ( $q_{As(III)} = 0.6719C_{NaCl} + 16.91$ ,  $R^2 = 0.9387$ ;  $q_{As(V)} = 0.614 C_{NaCl} + 17.679$ ,  $R^2 = 0.9584$ ). When NaCl increases from 0 to 2mol/L, the adsorption amount of As(III) and As(V) increase from 16.74 and 17.52 mg/g to 18.13 and 18.84 mg/g respectively, and the extent of As(III) adsorbed increasing is more than that of As(V).

As the adsorption competition on MIO surface between  $Cl^-$  and arsenic anion, it is disadvantageous to arsenic adsorption with the ionic strength of background electrolyte NaCl increasing [10].

According to Gouy-Chapman formula, the surface potential of MIO particulate is  $\phi_0$ :

$$\phi_0 = \phi_s + \zeta,$$

where  $\phi_s$  is the Stern layer potential and  $\zeta$  is the diffusion layer potential.

$\phi_0$  keeps constant in a certain pH,  $\phi_s$  and  $\zeta$  change as the double electric layer compressed for increasing electrolyte concentration [11]. According to this formula, the surface positive charge of MIO slightly increases as an increasing ion strength increases at pH 7.0, which is advantageous to arsenic adsorption. The ion strength had different effects on As(III) and As(V), indicating other mechanism may exist.

### 3.5. Effect of temperature on As(III) and As(V) adsorption on MIO

As arsenic is widely found in hot well water, it is necessary to investigate the effect of temperature on arsenic removal-adsorption. Fig. 6 shows the effect of temperature on arsenic adsorbed by MIO. The amount of As(III) and As(V) adsorbed by MIO obviously decreases with temperature from 20 to 60°C, As(III)

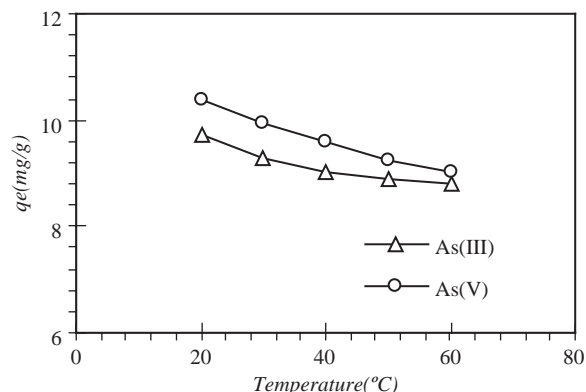


Fig. 6. Effects of temperature on arsenic adsorption. The ionic strength of background electrolyte NaCl is 0.1 mol/L, the solution pH is 7.0 and the added arsenic is 20 mg/L.

and As(V) from the adsorption of 9.74 and 10.40 mg/g to 8.80 and 9.04 mg/g, the extent of adsorption decreasing are 0.4 and 2.3 mg/g, respectively, and the decreasing extent of As(V) adsorption is higher than that of As(III). The results indicate that the adsorption process of arsenic is exothermic reaction. Arsenic is adsorbed by the coexistence heterogeneous oxides of MIO, and the adsorption process is non-homogeneous reaction. Under the conditions of this experiment at pH 7.0, iron oxide has variable positive charge (the PZC of iron oxide was more than 7.0). As seen from the Gouy-Chapman formula [11]: Surface potential  $\phi_0$ :

$$\phi_0 = \frac{2.303kT}{e} (\text{pH}_0 - \text{pH})$$

Surface charge density  $\sigma_0$ :

$$\sigma_0 = \left[ \frac{2N\epsilon kT}{\pi} \right]^{1/2} \sinh 1.5z(\text{pH}_0 - \text{pH})$$

where  $T$  is absolute temperature (K),  $K$  is Boltzmann constant ( $1.38 \times 10^{-23}$  J/K),  $e$  is electric charge ( $1.602 \times 10^{-19}$  coulomb),  $N$  is avogadro's number ( $6.02 \times 10^{23}$  /mol),  $\epsilon$  is dielectric constant and  $Z$  is ion value. Therefore, the surface charge density and potential increase with an increasing temperature, which is beneficial to arsenic adsorption on the iron oxide and promote the adsorption of arsenic on MIO.

## 4. Conclusions

MIO can effectively remove arsenic from aqueous solution via adsorption. It was slight difference between the adsorption capacity of MIO for As(V) and As(III), and has 3.6 mg/g higher adsorption capacity for As(V) than As(III) according to Langmuir equation

prediction. The adsorption was effected by pH, ionic strength and temperature. The optimal pH for As(III) adsorption is in the range of 6–9.4, and under acidic conditions for As(V). Arsenic adsorption increased with an increasing of ionic strength and a decreasing of temperature. Adsorbed arsenic could be effectively removed using 10% NaOH solution, and the desorption proceeds to a completion very fast. In 5 min the amount of arsenic desorption reaches 60–80%, while As(V) desorption was more easier than that of As(III).

### Acknowledgment

We gratefully thank the National Nature Science Foundation of China (No.50576078) for financial support to this research. Comments from anonymous reviewers significantly improved the manuscript too.

### References

- [1] J.Q. Jiang, Removing arsenic from groundwater for the developing world—a review. *Water Sci. Technol.*, 44 (6) (2001) 89–98.
- [2] X. Sun and H.E. Doner, An investigation of arsenate and arsenite bonding structures on goethite by FTIR. *Soil Sci.*, 161 (1996) 865–872.
- [3] C.M. Su and R.W. Puls, Arsenate and Arsenite removal by zerovalent iron: effects of phosphate, silicate, carbonate, borate, sulfate, chromate, molybdate, and nitrate, relative to chloride. *Environ. Sci. Technol.*, 35 (2001) 4562–4568.
- [4] L.C. Roberts, S.J. Hug, T. Ruettimann, A.W. Khan and M.T. Rahman, Arsenic removal with iron(II) and iron(III) in waters with high silicate and phosphate concentrations. *Environ. Sci. Technol.*, 38 (2004) 307–315.
- [5] X.Y. Wang, G.Q. Yang, L.M. Yan et al. The synthesis of  $MnFe_2O_4$  nanocrystals and their characterization. *Chem. Ind. Eng.*, 21 (2) (2004) 84–87.
- [6] D.L. Johnson and M.E.Q. Pilon, Spectrophotometric determination of arsenite, arsenate and phosphate in natural waters. *Anal. Chim. Acta*, 58 (1972) 289–299.
- [7] APHA-AWWA, 1985. *Standard Methods for the Examination of Water and Wastewater*, 16th ed. Am. Publ. Hlth Assoc. Am. Wat. Works Assoc., Washington, DC, USA.
- [8] Z.W. He and Y. Yang, Crystal chemistry of spinel-type structures. *Acta Mineral. Sini.*, 17(3) (1997) 321–328.
- [9] A. Jain, K.P. Raven and R.H. Loeppert, Arsenite and Arsenate adsorption on ferrihydrite: surface charge reduction and net  $OH^-$  release stoichiometry. *Environ. Sci. Technol.*, 33 (1999) 1179–1184.
- [10] X.G. Meng, G.P. Korfiatis, S. Bang and K.W. Bang, Combined effects of anions on arsenic removal by iron hydroxides. *Toxicol. Lett.* 133 (2002) 103–111.
- [11] G.Q. Liu, W.F. Tan, X.H. Feng, et al. The characteristics of Cr(III) oxidation by several Fe-Mn nodules in soils II. Effect of pH, ionic strength and temperature. *Acta Pedol. Sini.* 40 (6) (2003) 852–857.
- [12] J.S. Noh and J.A. Schwarz, Effect of  $HNO_3$  treatment on the surface acidity of activated carbons. *Carbon* 28(5) (1990) 675–682.